Title

A phase II evaluation of the potent, highly selective PARP inhibitor veliparib in the treatment of persistent or recurrent epithelial ovarian, fallopian tube, or primary peritoneal cancer in patients who carry a germline BRCA1 or BRCA2 mutation - An...

Permalink

Journal

ISSN

Authors

Coleman, Robert L
Sill, Michael W
Bell-McGuinn, Katherine
et al.

Publication Date

DOI

Evaluating visual perception for assessing reconstructed flap health

Adrien Ponticorvo, Ph.D.[1], **Eren Taydas, M.D.**[1], **Amaan Mazhar, Ph.D.**[2], **Christopher L. Ellstrom, M.D.**[3], **Jonathan Rimler, M.D.**[3], **Thomas Scholz, M.D.**[3], **June Tong**[1], **Gregory R.D. Evans, M.D.**[3], **David J. Cuccia, Ph.D.**[2], and **Anthony J. Durkin, Ph.D.**[1]

Anthony J. Durkin: adurkin@uci.edu

[1]Beckman Laser Institute and Medical Clinic, University of California Irvine, 1002 Health Sciences Road East, Irvine, CA 92617, USA

[2]Modulated Imaging Inc., Beckman Laser Institute Photonic Incubator, 1002 Health Sciences Rd. East, Irvine, CA. 92617, USA

[3]Department of Plastic Surgery, University of California Irvine Medical Center, 200 S. Manchester Ave., Suite 650, Orange, CA 92868, USA

Abstract

Background—Detecting failing tissue flaps before they are clinically apparent has the potential to improve post-operative flap management and salvage rates. This study demonstrates a model to quantitatively compare clinical appearance, as recorded via digital camera, with spatial frequency domain imaging (SFDI), a non-invasive imaging technique utilizing patterned illumination to generate images of total hemoglobin and tissue oxygen saturation.

Methods—Using a swine pedicle model where blood flow was carefully controlled with occlusion cuffs and monitored with ultrasound probes, throughput was reduced by 25%, 50%, 75%, and 100% of baseline values in either the artery or the vein of each of the flaps. The color changes recorded by a digital camera were quantified in order to predict which occlusion levels

---

Correspondence to: Anthony J. Durkin, `adurkin@uci.edu`.

were visible to the human eye. SFDI was also used to quantify the changes in physiological parameters including total hemoglobin and oxygen saturation associated with each occlusion.

Results—There were no statistically significant changes in color above the noticeable perception levels associated with human vision during any of the occlusion levels. However there were statistically significant changes in total hemoglobin and tissue oxygen saturation levels detected at the 50%, 75%, and 100% occlusion levels for arterial and venous occlusions.

Conclusion—As demonstrated by the color imaging data, visual flap changes are difficult to detect until significant occlusion has occurred. SFDI is capable of detecting changes in total hemoglobin and tissue oxygen saturation as a result of partial occlusions before they are perceivable, thereby potentially improving response times and salvage rates.

Keywords

spatial frequency domain imaging; flap reconstruction; color perception

1. Introduction

Free flap reconstruction is often utilized to repair a variety of complex defects. Success rates in free tissue transfer are reported to be between 91–99% at major microsurgical centers[1–6]. Between 5–25% of free flaps are reported to undergo re-exploration for microvascular compromise or other factors of which 37–81% are successfully salvaged[3, 5, 6]. One potential reason for lower salvage rates may be the delay in determining when flaps are failing since externally visible signs of microvascular compromise often lag behind the inciting event. Numerous studies have demonstrated that earlier detection and intervention for failing flaps is associated with improved outcomes[3, 5]. Partial occlusions are particularly difficult to detect and can have significant effects on flow dynamics with only subtlety apparent changes via conventional monitoring. Few animal studies focus on studying these partial occlusions[7], yet the ability to detect these early stages of occlusion may be critical for improving salvage rates in compromised tissue flaps[4, 5, 8].

Many modalities have been developed in an attempt to provide optimal free flap monitoring, however clinical bedside monitoring is the only ubiquitous standard[4]. Characteristics such as temperature, capillary refill rate, Doppler signal and color as well as the change of these parameters over time are utilized to determine when to take a flap back for exploration[4, 7, 9]. In order to provide a more quantitative evaluation, several studies have begun to investigate additional techniques to study tissue flaps. Laser Doppler has been used successfully in animals to detect partial occlusions[10], and Doppler ultrasound has been used to monitor tissue flaps post operatively in humans[11, 12]. Near-infrared spectroscopy (NIRS) has also proven to be useful in identifying occlusions in animals[13–15] and monitoring humans in a clinical setting[6, 16]. The main drawback to point measurement based techniques is their lack of ability to identify small problem areas over a large area of tissue. The use of imaging techniques like NIR fluorescence imaging allows perfusion levels in the entire flap to be monitored at once[17]. The drawback of this technique is the need to inject a contrast agent like indocyanine green (ICG) each time the target tissue needs to be examined. This can add additional cost and is not ideal for frequent scheduled monitoring

due to the limited half-life of the contrast. Spatial frequency domain imaging (SFDI) has been used to effectively quantify physiological parameter changes in flaps[18, 19] during complete[14, 20] and partial[21] vascular occlusions. It is an ideal tool for studying tissue flaps because it is a non-contact technique capable of quickly acquiring wide field data without the need for an exogenous contrast agent. While all of these techniques have been used with varying levels of effectiveness to study tissue flaps, it is difficult to measure how much benefit they provide beyond what can be assessed by basic human monitoring. This is largely because human monitoring is inherently subjective.

One aspect of human monitoring that is possible to quantify is the color changes associated with a failing flap. Quantifiable approaches to monitor color changes are typically done using point measurement colorimeters, although not prominent in examining flaps, they are commonly used to analyze scars[22, 23], port-wine stains[24], and pigmented lesions[25, 26]. Recent studies have shown that digital photography can yield similarly effective results to colorimeters when analyzed appropriately[26, 27]. This is often done by first normalizing the color images to a standard scale (typically CIELAB) and then interpreting differences in that new scale to quantify changes in color (E). As larger values of E represent large changes in color, it is feasible to set a minimum value of DE where human vision can begin to perceive changes in color. This is often referred to as the just noticeable difference (JND), but because perceivable color differences are not perfectly uniform throughout the CIELAB color space, most researchers agree that the JND can be between 1 and 3[28–31]. Studies that have focused on looking at color changes in the skin have claimed a E below 3 is unnoticeable[32]. In this study we quantified the color changes associated with swine tissue flaps undergoing different levels of partial occlusion to see when they would become noticeable, and compared these results with SFDI in order to more practically assess the benefit of this imaging technique for studying tissue flaps. While there are limitations in all animal models, human skin is closer to pig skin than any other readily available animal. This is because of similarities in thickness, structure, hair follicles, sweat glands, and subcutaneous fat [33]. However, the lack of pigment in Yorkshire pigs does minimize potential real world complications associated with optical imaging techniques like SFDI.

2. Methodology

These experiments were performed under University of California, Irvine Institutional Animal Care Use Committee approved protocol #2006-2693. Eight yorkshire pigs (30–50kg) were anesthetized with an intramuscular injection of ketamine (20mg/kg) and xylazine (2mg/kg), and an intravenous injection of pentobarbital (10mg/kg). The pigs were mechanically ventilated with oxygen (100%) and isoflurane (1–1.5%) and body temperature (36–38°C) was maintained with a heating pad. Bilateral 12cm × 7cm fasciocutaneous pedicled flaps based on the deep inferior epigastric vessels were raised in the abdominal area. In order to ensure that only one set of vessels would be connected to the flap, all of the vasculature between the femoral artery and vein and the flap was ligated except for the branches that led through the deep inferior epigastric artery and vein. A programmable syringe pump (NE-1000, New Era, Farmingdale, NY) injected saline into an occlusion balloon cuff (Docxs Biomedical, Ukiah, CA) causing it to inflate and restrict blood flow while an ultrasound probe (TS-420, Transonic System, Ithaca, NY) monitored blood flow.

This surgical procedure was performed on both flaps so that one could be used as a control. In four of the animals, the occlusion balloon and flow monitor were attached to the deep inferior epigastric artery (typical diameter around 3mm) as seen in Fig. 1(b). In the other four animals, these devices were attached to the deep inferior epigastric vein (typical diameter around 6mm). Approximately 60 minutes after the flap was sutured back into place, baseline blood flow was established in both flaps. In order to create a series of partial occlusions, the occlusion cuff was programmed to inflate until blood flow was reduced by 25% of the baseline value and maintained for 30 minutes. The occlusion cuff was then deflated for 30 minutes allowing the tissue flap to recover. This process was repeated for flow reductions of 50%, 75%, and 100% of the baseline values. Specified flow levels were typically reached within four minutes. The blood flow changes recorded during a typical experiment for partial occlusions of an arterial and venous vessel are shown in Fig. 1(c,d).

The setup for the imaging instrumentation has been described elsewhere[34], but a brief overview is provided. A prototype clinic-compatible system (v100, Modulated Imaging Inc., Irvine, CA) was used to collect the flap data. The imaging instrument consists of two cameras that alternately collected data; a near-infrared (NIR) camera (LU160m, Lumenera Corp., Ottawa, Canada) that was used for SFDI and a color camera (LU160c, Lumenera Corp., Ottawa, Canada) that was used to collect images for color analysis. Both cameras were co-registered to look at the same field of view and cross-polarizers were used to reduce specular reflection. In addition to the camera, SFDI requires a light source to be projected using a spatial light modulator to create spatially modulated illumination. Based on previous work[35], LED's centered at 658, 730, and 850 nm were used as the light source and a Digital Micromirror Device (Discovery™ 3000, Texas Instruments Inc., Dallas, TX) was used as a spatial light modulator. The field of view of both cameras is approximately 13.5cm × 10.5cm. For SFDI a sinusoidal pattern of two frequencies (0 and 0.2mm^{-1}) was projected at three phases (0, 120, and 240 degrees) by each of the LEDs. Immediately prior to this series of patterns, white light was projected to capture a digital color image, a surrogate for clinical impression, for later analysis. It took approximately 12s to collect one sequence of data, and this process was synchronized with the ventilator and repeated approximately every 30s. Custom C# software (Modulated Imaging Inc., Irvine, CA) was used to control the hardware. A schematic of the instrumentation is shown in Fig. 2.

MATLAB (R2011b, Mathworks, Natick MA) was used to convert color images from the digital camera to CIELAB images. Images were first transformed from red, blue, green (RGB) to the CIE 1931 XYZ color space and then were converted to the traditional CIE 1976 (L*, a*, b*) color space using CIE standard illuminant D65 as a reference point. Once each pixel of the image was represented in the L*, a*, b* color space and a baseline image was established to compare the pixel value at a given time point with the same pixel in the baseline image, a E image was created at each time point using Equation 1 below. The E formula essentially represents the distance between two points in the L*, a*, b* color space where larger distances represent larger and more noticeable color differences below[28–32].

$$\Delta E_{ab}^* = \sqrt{(L_1^* - L_2^*)^2 + (a_1^* - a_2^*)^2 + (b_1^* - b_2^*)^2} \quad (1)$$

Custom software was written in MATLAB to analyze the SFDI data has been described previously[34]. For each spatial frequency, the demodulation of the three phases was used to determine the AC component of the reflected image. Demodulated reflectance values were used to estimate the absorption and reduced scattering coefficient properties based on a scaled Monte Carlo generated lookup table at each wavelength[36]. Precise positioning is not a prerequisite for obtaining data using the SFDI system. In general, the system used to collect the data can accommodate variations up to 7cm. Research has been done on algorithms related to height correction[37] and motion correction[38] to improve the images for the SFDI system. Several advances have also been made to acquire images in seconds to further limit the impact of motion. A surface profilometry calibration measurement of a sample with known optical properties was used to correct for the effects of surface curvature[37]. The absorption coefficient maps were used to generate chromophore concentration maps of oxygenated and deoxygenated hemoglobin that could be converted to total hemoglobin (ctTHb) by summing the two, or tissue oxygen saturation (stO_2) by dividing oxygenated hemoglobin by total hemoglobin. Changes in total hemoglobin (ΔctTHb) and tissue oxygen saturation (ΔstO$_2$) were calculated relative to each animal's respective baseline hemodynamic SFDI data. In order to analyze parameter values in every tissue flap, a homogeneous region of interest (ROI) devoid of large vessels near the center of each flap, approximately 2cm × 2cm, was chosen so that values in that region could be averaged together.

In order to assess whether there was a statistically significant change in the color of each flap, a one-tailed, one sample student's t-test was used to see if changes in color (ΔE) were above the JND level of 3 at each occlusion level (25%-100%). Similarly, parameters like stO_2 and ctTHb that were derived using SFDI, were tested for significance by comparing measured changes to baseline values. These tests were done by using the averaged parameter values in the ROI at a time point in the middle of the occlusion, and then averaged across all animals in the same group. A p-value less than 0.05 was considered significant for this study.

3. Results

To highlight the variability that was observed among animals during the series of partial venous occlusions, Fig. 3 and Fig. 4 show a montage of images from the experiments that exhibited the largest and smallest color changes respectively. Each collection of images presents the color images along with the ΔE and the ΔctTHb images overlayed with those same color images at different time points. The time points correspond to the baseline images as well as at the mid-point of each occlusion level. In order to better visualize the parameters, the ΔE images are thresholded so that only values above 3 are displayed to emphasize the JND. Similarly, the ΔctTHb images are thresholded so that only changes above 5% are shown in order to avoid seeing smaller, potentially noise related fluctuations.

The venous occlusion experiment with the most statistically significant color changes (Fig. 3) at the 100% occlusion level (no measureable flow) also had noticeable color changes at the 75% level, but no noticeable changes at the smaller occlusion levels beyond those seen

in a large vein. The ctTHb changes on the other hand could be seen throughout the flap at each occlusion level.

The venous occlusion experiment with the least statistically significant color changes (Fig. 4) at the 100% occlusion level had spatially scattered changes at that level with almost no perceivable change at the 75% level. Despite this, changes in ctTHb could be seen throughout the majority of the flap at the 100%, 75%, and 50% occlusion levels.

The time courses of both parameters in a given ROI for each partial venous occlusion experiment in addition to the average values with error bars (standard deviation) are shown in Fig. 5. There were no statistically significant changes above the JND in ΔE at any of the occlusion levels. At the 100% occlusion level, values for ΔE varied from above 14 to below the JND of 3. No changes in color were noticeable at the 25% or 50% occlusion level in any of the animals. However, there were statistically significant increases in ctTHb above the average baseline values at the 100%, 75%, and 50% occlusion levels.

A similar montage of images from a typical arterial occlusion experiment is shown in Fig. 6. There are noticeable changes throughout the flap at the 100% occlusion level and some noticeable changes at the 75% level. Changes in stO$_2$ could be seen throughout the majority of the flap at all occlusion levels.

The time courses of ΔE and stO$_2$ for a given ROI in each partial arterial occlusion experiment in addition to the average values with error bars (standard deviation) are shown in Fig. 7. Statistically significant stO$_2$ changes were seen at the 50%, 75%, and 100% occlusion levels. There were no statistically significant ΔE changes at any of the occlusion levels. There were a wide range of values for ΔE at the 100% occlusion level that ranged from above 7 to just below the JND. At the partial occlusion levels, no color changes were above the JND.

4. Discussion

Using an animal model that carefully controls blood flow to isolated tissue flaps allows us to study the effects of partial occlusions and carefully evaluate various aspects related to detecting flap compromise. In patients these partial occlusions may eventually lead to complete occlusions and subsequent flap failure. The capability to detect partial occlusions is significant because it implies potential to recognize flap dysfunction at relatively early postoperative time points. This is turn suggests improved potential for flap salvage[3, 5]. Several imaging and monitoring modalities have been utilized to attempt earlier detection of a compromised flap in the immediate postoperative period, but it is difficult to assess their effectiveness compared to conventional intermittent physical exams[5, 7]. Recent studies utilizing photography for remote flap monitoring have demonstrated that careful photographic evaluation of flap color and appearance may allow for more rapid identification of failing flaps with an accuracy of 94.7% compared to a rate of 98.7% for in person examination[39, 40]. Though these studies utilize flap color and appearance to demonstrate remote evaluations comparable to physical exam, the assessments are still largely subjective. Here we used a technique to quantify the human perception of color

changes, similar to what others have done with scars and pigmented lesions[22, 25], in order to examine the effectiveness of patient monitoring and compare it to results obtained using SFDI.

There was significant variability in the color changes seen from animal to animal for a given occlusion level. While most animals had noticeable flap color changes during complete 100% occlusions (no measurable blood flow) in the arterial and venous groups, there were some animals in both groups that did not. During the partial occlusion experiments most of the animals did not have noticeable changes in flap color. However, at the 75% occlusion level in the venous group, some changes in color were slightly above the JND line. Other groups using similar techniques in pigs have seen larger changes in color during occlusion[7], but this is probably attributed to the fact that they occluded the flaps for a much longer period of time. While it is likely that we could have created larger changes in color by extending occlusion times, ultimately we were interested in quantifying the ability of human observation to detect early signs of flap failure. We have previously shown the ability of SFDI to detect multiple physiological parameters related to the perfusion status of a given flap[21]. The use of those parameters, specifically ctTHb for monitoring venous occlusions and stO$_2$ for monitoring arterial occlusions, were significantly better at detecting changes in the flap. In addition to being more reliable at detecting changes at the 100% occlusion level, SFDI was also effective at detecting changes during the partial occlusions. When the data for this experiment was collected, it was analyzed at a later date, but the current version of the system can output results immediately after acquisition. The current standard of care is post-operative visual examination on an hourly basis. SFDI has the potential to be useful as a quantitative tool during this inspection.

It is important to note that the digital color camera used here was more effective at detecting flap color changes than unaided human perception. The camera was able to record changes below the JND threshold. This suggests the potential for cameras to not only be used for remote monitoring purposes, but also for actual analysis of flap health. One drawback to using digital color photography is that it is not effective at analyzing a flap at a single point in time. It must continuously monitor a flap with essentially calibrated, controlled lighting conditions and assumes that the baseline condition of the flap is healthy in order to be effective. Ultimately, the ability to monitor physiological parameters like oxygen saturation and total hemoglobin levels that are directly related to flap health are better indicators of early flap failure.

5. Conclusion

The clinical appearance of a free flap in the early postoperative period is not always representative of the underlying microvascular condition. As demonstrated by the color imaging data in our study, clinically apparent changes in flap color that are within the range of human detection are often not visible until significant vascular occlusion has occurred. Digital analysis of flap photos over time appears to be more sensitive in detecting changes compared human perception alone in a swine model. Further study should be done to determine the efficacy of this technique in a clinical setting. By comparison, SFDI is capable of detecting changes in tissue oxygen saturation as a result of partial blood flow occlusions

to pedicle flaps before they are visible to the human eye. The early detection of flaps with vascular compromise has the potential to improve response times and salvage rates, making photographic flap analysis and SFDI useful tools for free flap management.

Acknowledgments

References

1. Chubb D, Rozen WM, Whitaker IS, Acosta R, Grinsell D, Ashton MW. The efficacy of clinical assessment in the postoperative monitoring of free flaps: a review of 1140 consecutive cases. Plast Reconstr Surg. 2010; 125(4):1157–1166. [PubMed: 20335866]

2. Pohlenz P, Blessmann M, Blake F, Li L, Schmelzle R, Heiland M. Outcome and complications of 540 microvascular free flaps: the Hamburg experience. Clin Oral Inves. 2007; 11(1):89–92.

3. Chen K-T, Mardini S, Chuang DC-C, Lin C-H, Cheng M-H, Lin Y-T, Huang W-C, Tsao C-K, Wei F-C. Timing of presentation of the first signs of vascular compromise dictates the salvage outcome of free flap transfers. Plast Reconstr Surg. 2007; 120(1):187–195. [PubMed: 17572562]

4. Bui DT, Cordeiro PG, Hu Q-Y, Disa JJ, Pusic A, Mehrara BJ. Free flap reexploration: indications, treatment, and outcomes in 1193 free flaps. Plast Reconstr Surg. 2007; 119(7):2092–2100. [PubMed: 17519706]

5. Kroll SS, Schusterman MA, Reece GP, Miller MJ, Evans GR, Robb GL, Baldwin BJ. Timing of pedicle thrombosis and flap loss after free-tissue transfer. Plast Reconstr Surg. 1996; 98(7):1230–1233. [PubMed: 8942909]

6. Steele MH. Three-Year Experience Using Near Infrared Spectroscopy Tissue Oximetry Monitoring of Free Tissue Transfers. Ann Plast Surg. 2011; 66(5):540–545. [PubMed: 21301288]

7. Russell JA, Conforti ML, Connor NP, Hartig GK. Cutaneous Tissue Flap Viability following Partial Venous Obstruction. Plast Reconstr Surg. 2006; 117(7):2259–2266. [PubMed: 16772926]

8. Chan RK, Liu A, Bojovic B, Chun Y, Guo L, Caterson SA, Orgill DP, Pribaz JJ. Venous congestion in abdominal flap breast reconstructions--a simple treatment for a temporary problem. J Plast Reconstr Aesthet Surg. 2011; 64(5):135–136.

9. Chubb D, Whitaker IS, Rozen WM, Ashton MW. Continued Observations in the Postoperative Monitoring of Free Flaps. Plast Reconstr Surg. 2012; 129(1):222–223.

10. Gimbel ML, Rollins MD, Fukaya E, Hopf HW. Monitoring Partial and Full Venous Outflow Compromise in a Rabbit Skin Flap Model. Plast Reconstr Surg. 2009; 124(3):796–803. [PubMed: 19730298]

11. Lorenzetti F, Ahovuo J, Suominen S, Salmi A, Asko-Seljavaara S. Colour Doppler ultrasound evaluation of haemodynamic changes in free tram flaps and their donor sites. Scand J Plast Reconstr Surg Hand Surg. 2002; 36(4):202–206. [PubMed: 12426993]

12. Vakharia KT, Henstrom D, Lindsay R, Cunnane MB, Cheney M, Hadlock T. Color Doppler ultrasound: effective monitoring of the buried free flap in facial reanimation. Otolaryngol Head Neck Surg. 2012; 146(3):372–376. [PubMed: 22261491]

13. Thorniley MS, Sinclair JS, Barnett NJ, Shurey CB, Green CJ. The use of near-infrared spectroscopy for assessing flap viability during reconstructive surgery. Br J Plast Surg. 1998; 51(3):218–226. [PubMed: 9664881]

14. Pharaon MR, Scholz T, Bogdanoff S, Cuccia D, Durkin AJ, Hoyt DB, Evans GRD. Early Detection of Complete Vascular Occlusion in a Pedicle Flap Model Using Quantitation Spectral Imaging. Plast Reconstr Surg. 2010; 126(6):1924–1935. [PubMed: 21124132]

15. Yafi A, Vetter TS, Scholz T, Patel S, Saager RB, Cuccia DJ, Evans GR, Durkin AJ. Postoperative quantitative assessment of reconstructive tissue status in a cutaneous flap model using spatial frequency domain imaging. Plast Reconstr Surg. 2011; 127(1):117–130. [PubMed: 21200206]

16. Whitaker I, Pratt G, Rozen W, Cairns S, Barrett M, Hiew L, Cooper M, Leaper D. Near Infrared Spectroscopy for Monitoring Flap Viability Following Breast Reconstruction. J Reconstr Microsurg. 2011

17. Matsui A, Lee BT, Winer JH, Laurence RG, Frangioni JV. Quantitative Assessment of Perfusion and Vascular Compromise in Perforator Flaps Using a Near-Infrared Fluorescence-Guided Imaging System. Plast Reconstr Surg. 2009; 124(2):451–460. [PubMed: 19644259]

18. Nguyen JT, Lin SJ, Tobias AM, Gioux S, Mazhar A, Cuccia DJ, Ashitate Y, Stockdale A, Oketokoun R, Durr NJ, Moffitt LA, Durkin AJ, Tromberg BJ, Frangioni JV, Lee BT. A novel pilot study using spatial frequency domain imaging to assess oxygenation of perforator flaps during reconstructive breast surgery. Ann Plast Surg. 2013; 71(3):308–315. [PubMed: 23945533]

19. Nguyen TT, Ramella-Roman JC, Moffatt LT, Ortiz RT, Jordan MH, Shupp JW. Novel application of a spatial frequency domain imaging system to determine signature spectral differences between infected and noninfected burn wounds. J Burn Care Res. 2013; 34(1):44–50. [PubMed: 23292572]

20. Gioux S, Mazhar A, Lee BT, Lin SJ, Tobias AM, Cuccia DJ, Stockdale A, Oketokoun R, Ashitate Y, Kelly E, Weinmann M, Durr NJ, Moffitt LA, Durkin AJ, Tromberg BJ, Frangioni JV. First-in-human pilot study of a spatial frequency domain oxygenation imaging system. J Biomed Opt. 2011; 16(8):086015. [PubMed: 21895327]

21. Ponticorvo A, Taydas E, Mazhar A, Scholz T, Kim HS, Rimler J, Evans GR, Cuccia DJ, Durkin AJ. Quantitative assessment of partial vascular occlusions in a swine pedicle flap model using spatial frequency domain imaging. Biomed Opt Express. 2013; 4(2):298–306. [PubMed: 23412357]

22. Cheon YW, Lee WJ, Rah DK. Objective and quantitative evaluation of scar color using the L*a*b* color coordinates. J Craniofac Surg. 2010; 21(3):679–684. [PubMed: 20485028]

23. Li-Tsang CW, Lau JC, Liu SK. Validation of an objective scar pigmentation measurement by using a spectrocolorimeter. Burns. 2003; 29(8):779–784. [PubMed: 14636751]

24. Rah DK, Kim SC, Lee KH, Park BY, Kim DW. Objective evaluation of treatment effects on port-wine stains using L*a*b* color coordinates. Plast Reconstr Surg. 2001; 108(4):842–847. [PubMed: 11547137]

25. Kim SC, Kim DW, Hong JP, Rah DK. A quantitative evaluation of pigmented skin lesions using the L*a*b* color coordinates. Yonsei Med J. 2000; 41(3):333–339. [PubMed: 10957887]

26. Miyamoto K, Takiwaki H, Hillebrand GG, Arase S. Development of a digital imaging system for objective measurement of hyperpigmented spots on the face. Skin Res Technol. 2002; 8(4):227–235. [PubMed: 12423541]

27. Leon K, Mery D, Pedreschi F, Leon J. Color measurement in L*a*b* units from RGB digital images. Food Research International. 2006; 39(10):1084–1091.

28. Hill B, Roger T, Vorhagen FW. Comparative analysis of the quantization of color spaces on the basis of the CIELAB color-difference formula. Acm Transactions on Graphics. 1997; 16(2):109–154.

29. Stokes M, Fairchild MD, Berns RS. Precision Requirements for Digital Color Reproduction. Acm Transactions on Graphics. 1992; 11(4):406–422.

30. Ikeda H, Dai W, Higaki Y. A Study on Colorimetric Errors Caused by Quantizing Color Information. IEEE T Instrum Meas. 1992; 41(6):845–849.

31. Mahy M, Vanmellaert B, Vaneycken L, Oosterlinck A. The Influence of Uniform Color Spaces on Color Image-Processing - a Comparative-Study of Cielab, Cieluv, and Atd. Journal of Imaging Technology. 1991; 17(5):232–243.

32. Vander Haeghen Y, Naeyaert JM, Lemahieu I, Philips W. An imaging system with calibrated color image acquisition for use in dermatology. IEEE Trans Med Imaging. 2000; 19(7):722–730. [PubMed: 11055787]

33. Forbes PD. Radiation effects in swine. I. Vascular supply of the skin and hair. USNRDL-TR-67-141. Res Dev Tech Rep. 1967:1–18. [PubMed: 5300775]

34. Cuccia DJ, Bevilacqua F, Durkin AJ, Ayers FR, Tromberg BJ. Quantitation and mapping of tissue optical properties using modulated imaging. J Biomed Opt. 2009; 14(2):024012. [PubMed: 19405742]

35. Mazhar A, Dell S, Cuccia DJ, Gioux S, Durkin AJ, Frangioni JV, Tromberg BJ. Wavelength optimization for rapid chromophore mapping using spatial frequency domain imaging. J Biomed Opt. 2010; 15(6):061716. [PubMed: 21198164]

36. Erickson TA, Mazhar A, Cuccia D, Durkin AJ, Tunnell JW. Lookup-table method for imaging optical properties with structured illumination beyond the diffusion theory regime. J Biomed Opt. 2010; 15(3):036013. [PubMed: 20615015]

37. Gioux S, Mazhar A, Cuccia DJ, Durkin AJ, Tromberg BJ, Frangioni JV. Three-dimensional surface profile intensity correction for spatially modulated imaging. J Biomed Opt. 2009; 14(3):034045. [PubMed: 19566337]

38. Nguyen JQ, Saager RB, Cuccia DJ, Kelly KM, Jakowatz J, Hsiang D, Durkin AJ. Effects of motion on optical properties in the spatial frequency domain. J Biomed Opt. 2011; 16(12):126009. [PubMed: 22191926]

39. Engel H, Huang JJ, Tsao CK, Lin CY, Chou PY, Brey EM, Henry SL, Cheng MH. Remote real-time monitoring of free flaps via smartphone photography and 3G wireless internet: A prospective study evidencing diagnostic accuracy. Microsurgery. 2011; 31(8):589–595. [PubMed: 22072583]

40. Varkey P, Tan NC, Girotto R, Tang WR, Liu YT, Chen HC. A picture speaks a thousand words: the use of digital photography and the Internet as a cost-effective tool in monitoring free flaps. Ann Plast Surg. 2008; 60(1):45–48. [PubMed: 18281795]
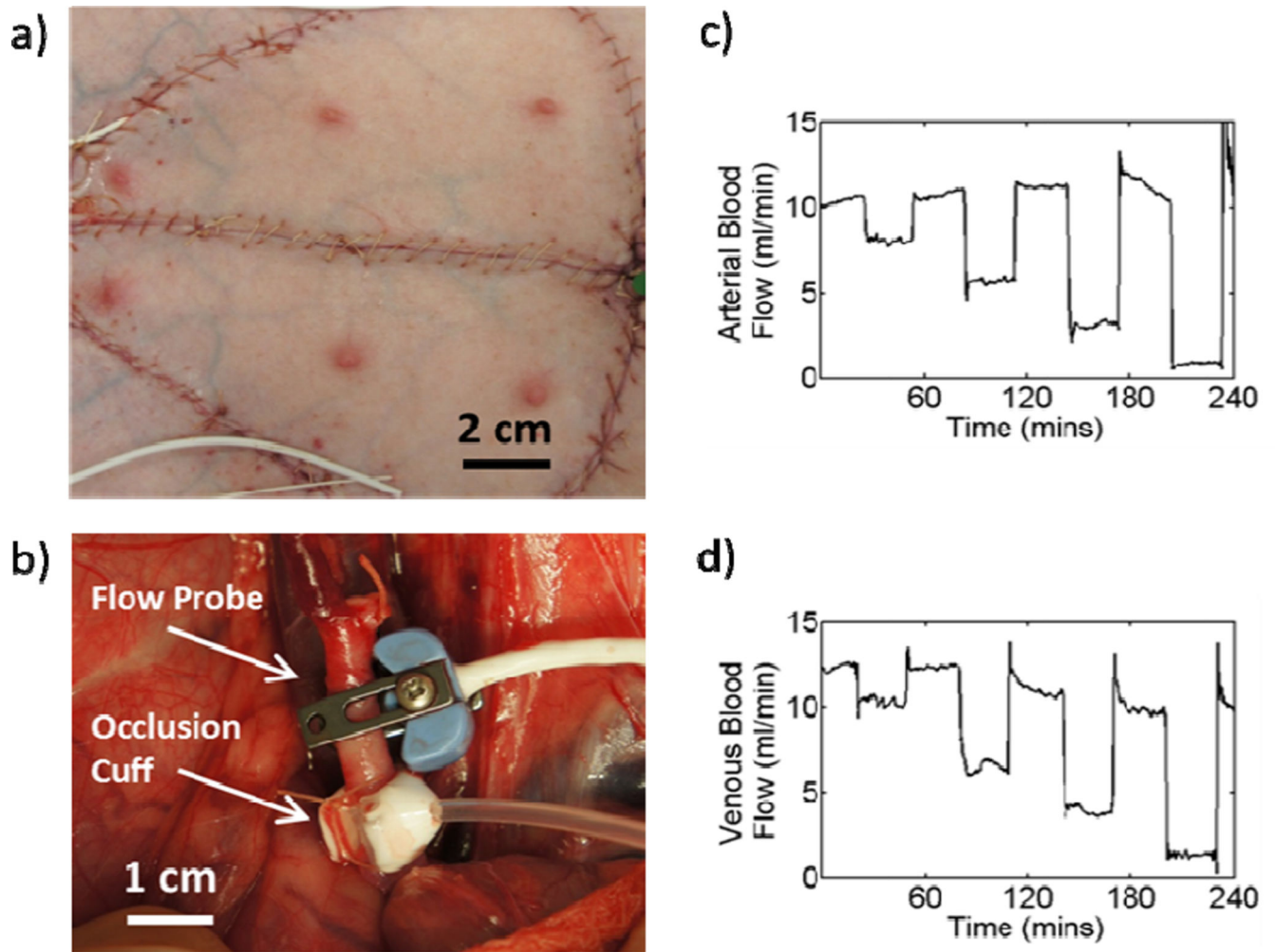
Fig 1.
Photograph of a) top view and b) underside of typical swine pedicle flap preparation with instrumentation labeled. Time course of blood flow changes during a series of typical c) arterial and d) venous partial occlusions.
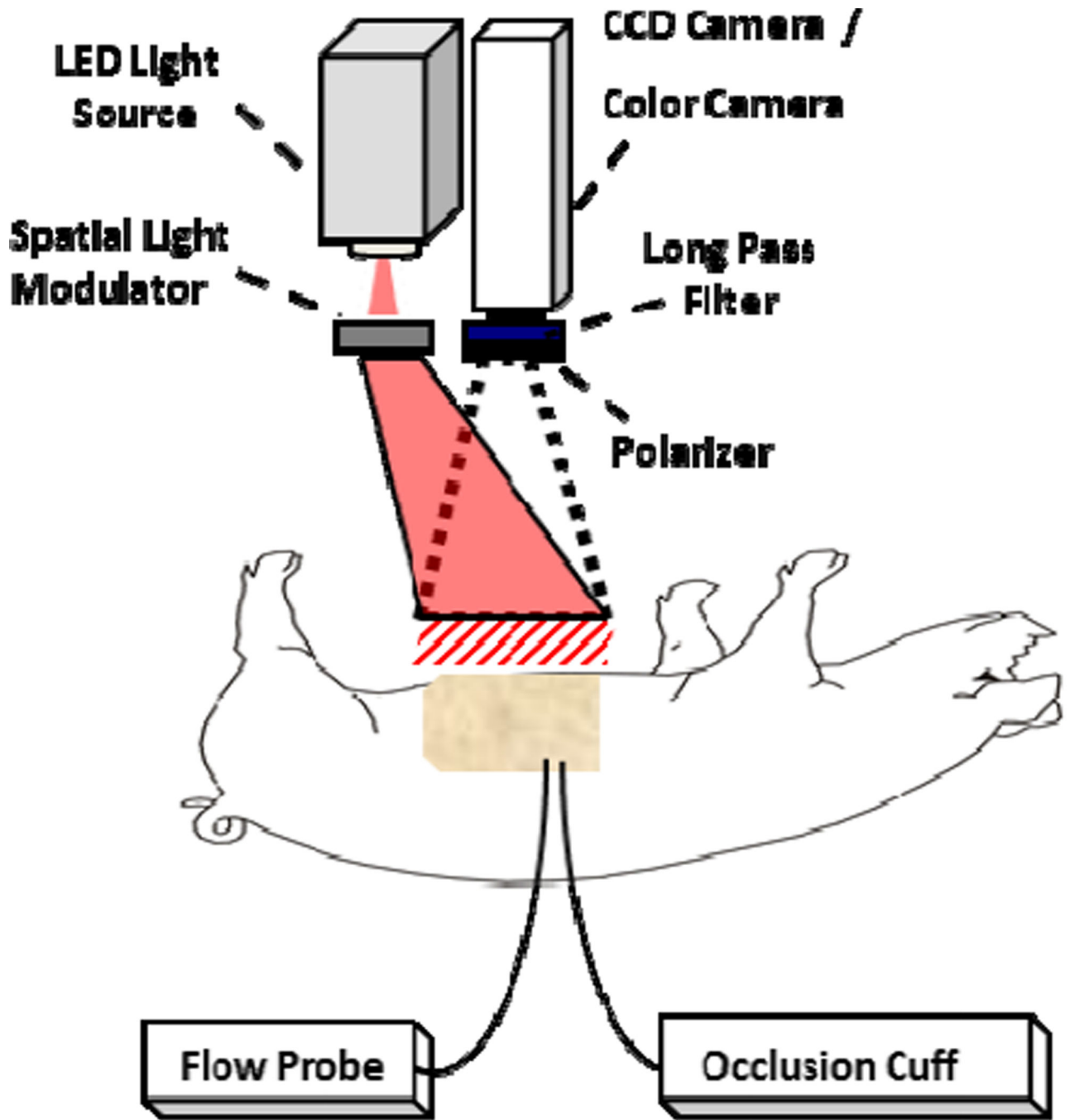
Fig 2.
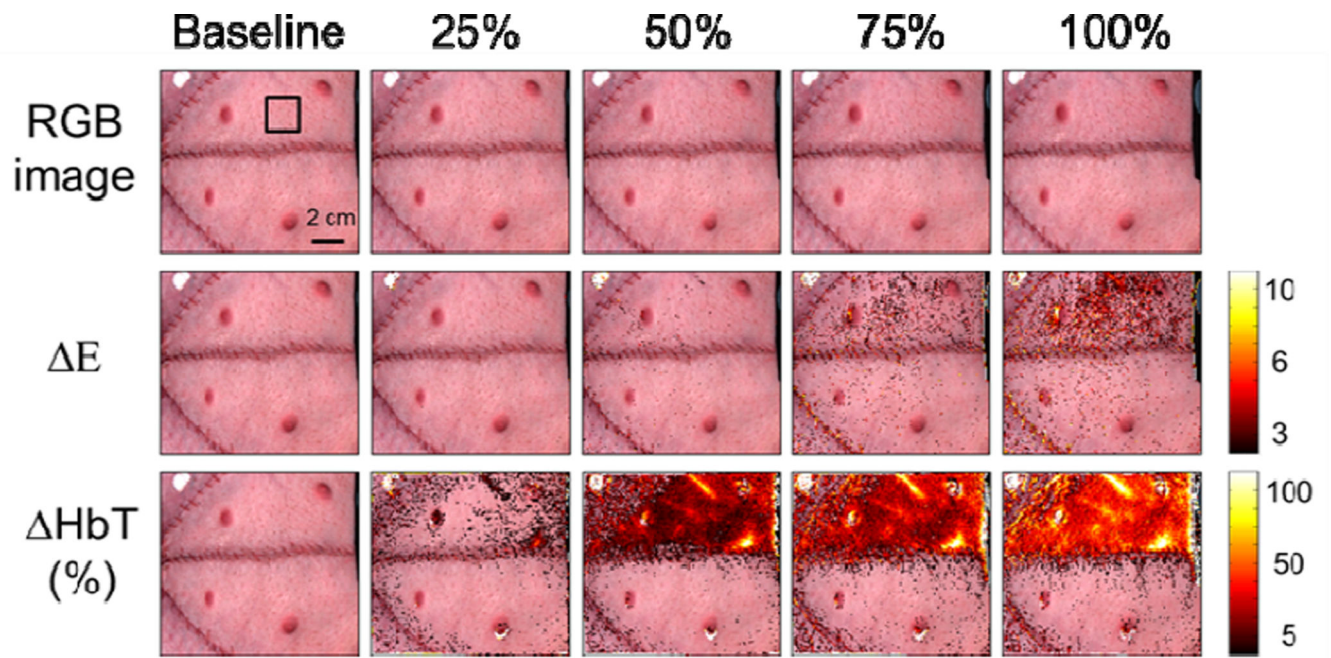Diagram of imaging system and feedback occlusion system.
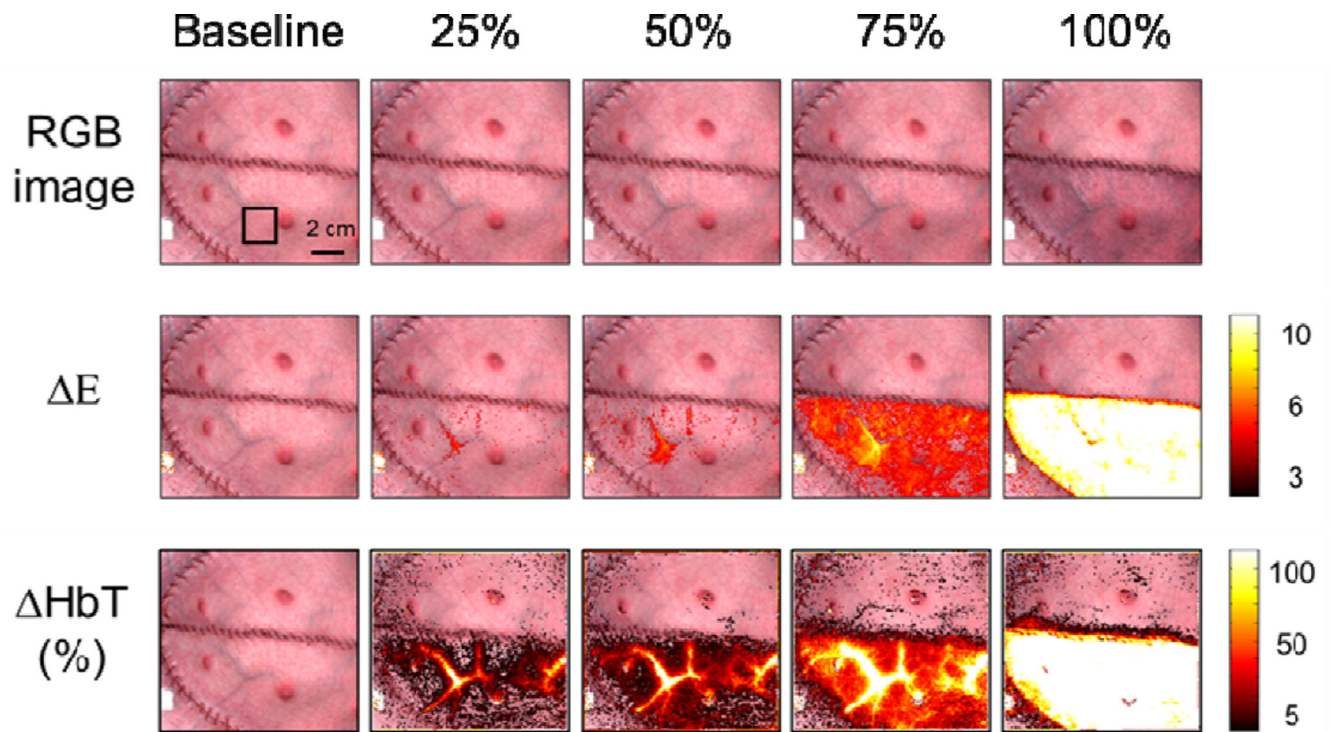
Fig. 3.
Color images, overlayed ΔE images, and overlayed ΔHbT images at different time points corresponding to different occlusion levels from a venous occlusion experiment that showed the most significant color changes.
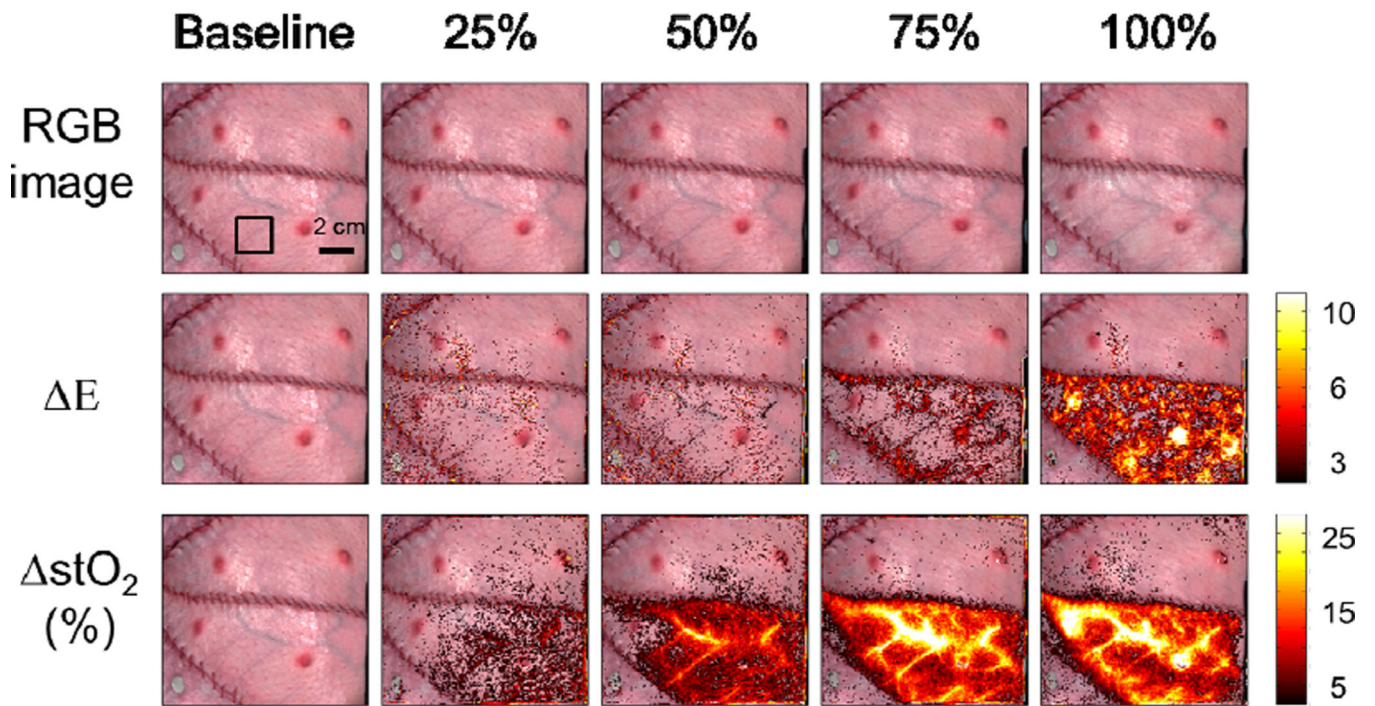
Fig. 4.
Color images, overlayed ΔE images, and overlayed ΔHbT images at different time points corresponding to different occlusion levels from a venous occlusion experiment that showed the least significant color changes.
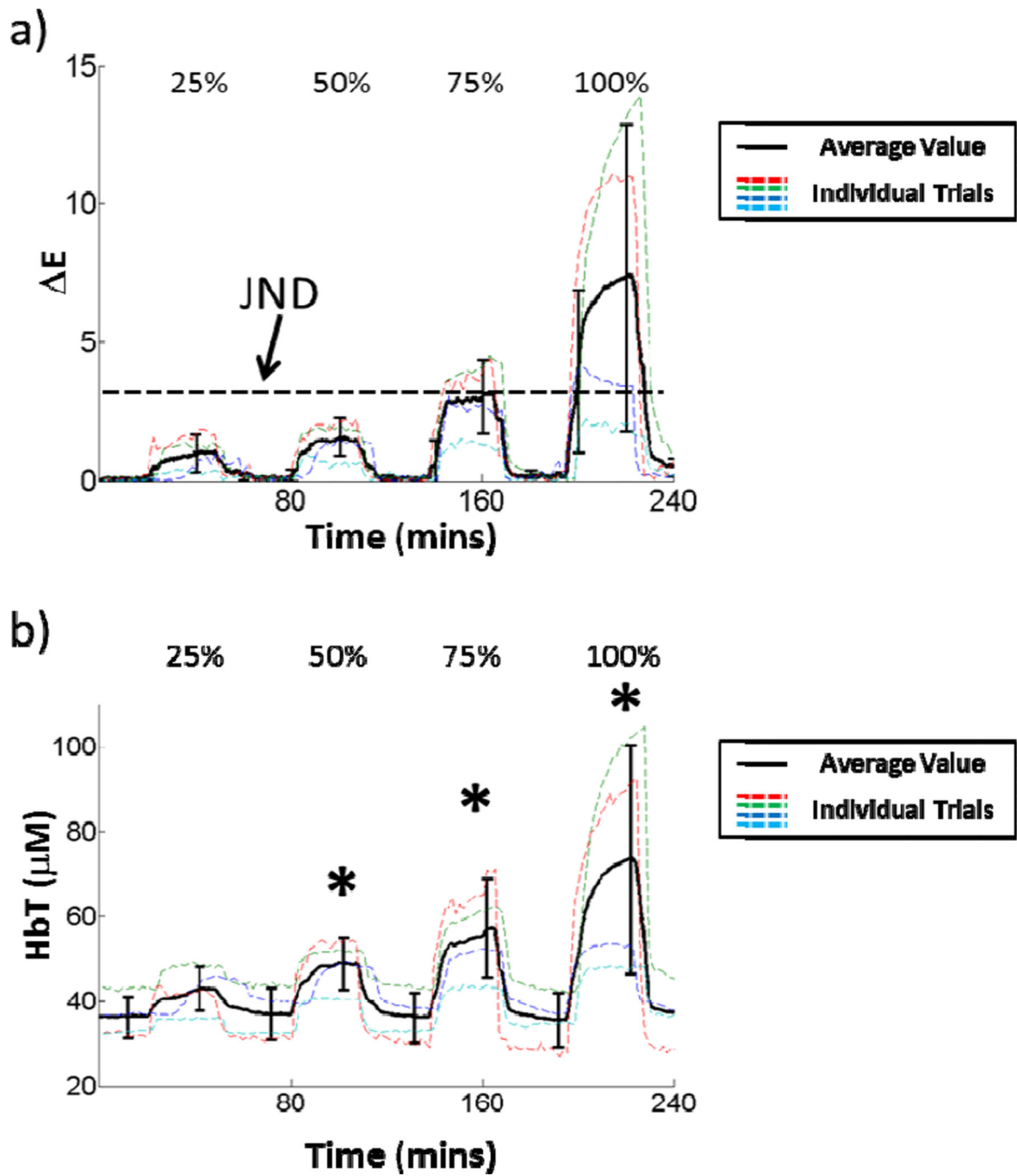
Fig. 5.
The time courses of a) E and b) HbT changes across all venous occlusion experiments. Statistically significant changes at a given occlusion level are marked with an asterisk.

Fig. 6.
Color images, overlayed ΔE images, and overlayed ΔstO$_2$ images at different time points corresponding to different occlusion levels from a typical arterial occlusion experiment.
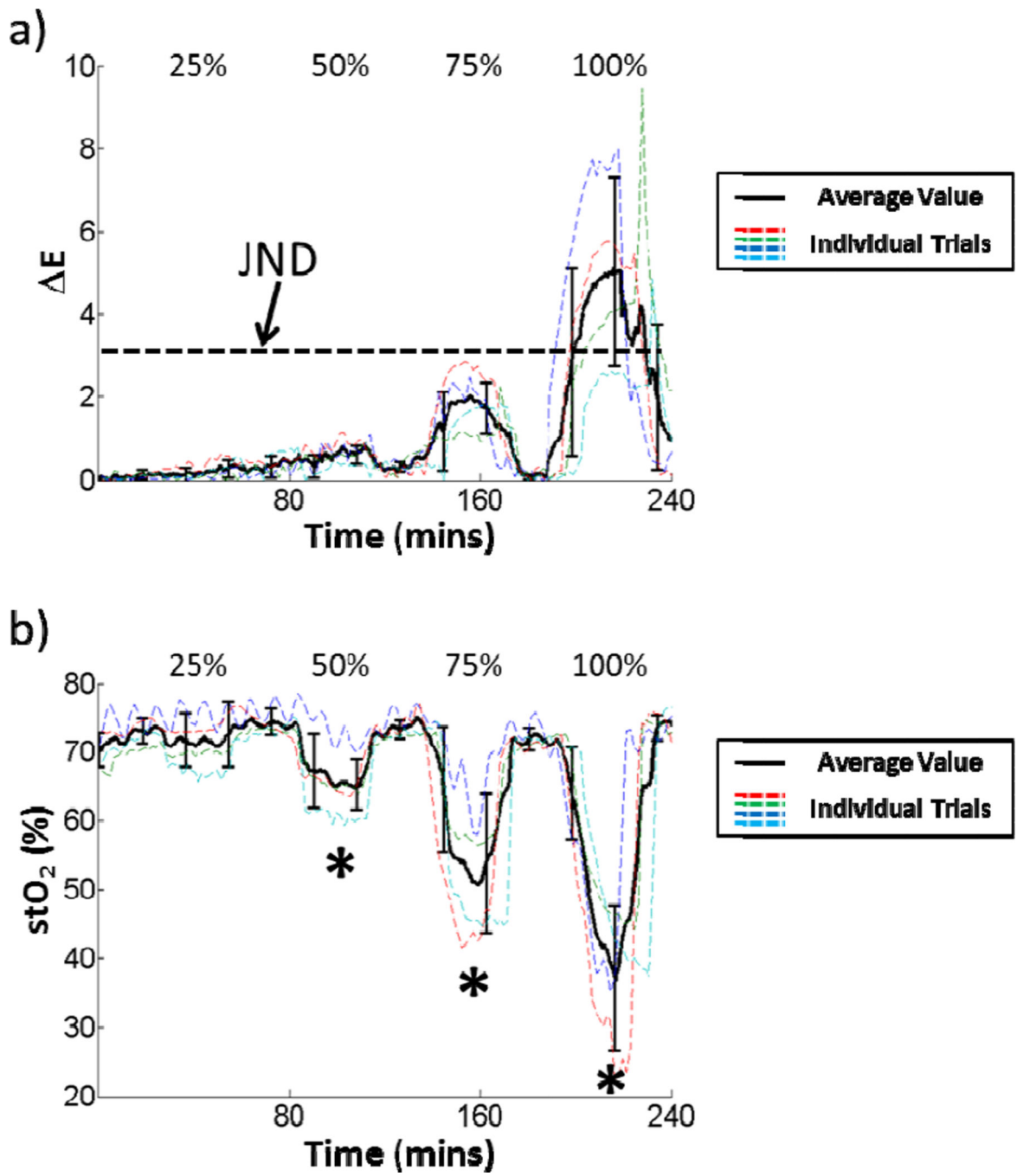
Fig. 7.
The time courses of a) E and b) stO$_2$ changes across all arterial occlusion experiments. Statistically significant changes at a given occlusion level are marked with an asterisk.